

---

# Bootstrap aggregation and confidence measures to improve time series causal discovery

---

**Kevin Debeire**

Deutsches Zentrum für Luft- und Raumfahrt (DLR)  
Institut für Physik der Atmosphäre,  
Oberpfaffenhofen, Germany.

and

Deutsches Zentrum für Luft- und Raumfahrt e.V. (DLR)  
Institut für Datenwissenschaften  
Jena, Germany.  
kevin.debeire@dlr.de

**Jakob Runge**

Deutsches Zentrum für Luft- und Raumfahrt e.V. (DLR)  
Institut für Datenwissenschaften  
Jena, Germany

and

Technische Universität Berlin  
Faculty of Computer Science  
Berlin, Germany.

**Andreas Gerhardus**

Deutsches Zentrum für Luft- und Raumfahrt e.V. (DLR)  
Institut für Datenwissenschaften  
Jena, Germany.

**Veronika Eyring**

Deutsches Zentrum für Luft- und Raumfahrt (DLR)  
Institut für Physik der Atmosphäre,  
Oberpfaffenhofen, Germany.

and

University of Bremen  
Institute of Environmental Physics (IUP)  
Bremen, Germany.

## Abstract

Causal discovery methods have demonstrated the ability to identify the time series graphs representing the causal temporal dependency structure of dynamical systems. However, they do not include a measure of the confidence of the estimated links. Here, we introduce a novel bootstrap aggregation (bagging) and confidence measure method that is combined with time series causal discovery. This new method allows measuring confidence for the links of the time series graphs calculated by causal discovery methods. This is done by bootstrapping the original times series data set while preserving temporal dependencies. Next to confidence measures, aggregating the bootstrapped graphs by majority voting yields a final aggregated output graph. In this work, we combine our approach with the state-of-the-art

conditional-independence-based algorithm PCMCI+. With extensive numerical experiments we empirically demonstrate that, in addition to providing confidence measures for links, Bagged-PCMCI+ improves the precision and recall of its base algorithm PCMCI+. Specifically, Bagged-PCMCI+ has a higher detection power regarding adjacencies and a higher precision in orienting contemporaneous edges while at the same time showing a lower rate of false positives. These performance improvements are especially pronounced in the more challenging settings (short time sample size, large number of variables, high autocorrelation). Our bootstrap approach can also be combined with other time series causal discovery algorithms and can be of considerable use in many real-world applications, especially when confidence measures for the links are desired.

## 1 INTRODUCTION

Since a rigorous mathematical framework for causal analyses has been established in the seminal works of Pearl, Spirtes, Glymour, Scheines, and Rubin [Imbens and Rubin, 2015, Pearl, 2009, Spirtes et al., 2000, Rubin, 1974], causal inference has undergone continuous developments to address the challenges of real-world problem settings. Learning causal graphs from data (termed causal discovery) is a main pillar of causal inference and of high interest in many fields where not even qualitative causal knowledge in the form of graphs is available, such as in biology [Friedman et al., 2000], neuroscience [Kaminski et al., 2001], or Earth system sciences [Nowack et al., 2020, Galytska et al., 2022 (in review, Karmouche et al., 2023)]. Furthermore, data in these fields typically comes in the form of time series, constituting a more general problem setting than the standard *i.i.d.*-case. In [Runge et al., 2019a], the authors give an overview of a few main categories of **time series causal discovery** methods: Granger causality and its extensions [Granger, 2001], nonlinear state-space methods (CCM [Sugihara et al., 2012]), causal network learning algorithms (for example, naive adaptations of the PC-algorithm [Spirtes and Glymour, 1991], PCMCI and its extensions like PCMCI+ [Runge et al., 2019b, Runge, 2020, Gerhardus and Runge, 2020], FCI [Spirtes et al., 2000, Zhang, 2008]), Bayesian score-based approaches [Chickering, 1996], and the structural causal model framework (VarLiNGAM [Hyvärinen et al., 2010]).

In parallel with the development of causal discovery methods, Breiman [1996] introduced **bootstrap aggregation** (bagging) which has initially been used to improve the accuracy and stability of machine learning algorithms. In bagging, a random sample in the training set is selected with replacement—meaning that each data point can be drawn more than once. Several data samples are generated in this fashion to produce a set of replicates (also called resamples). The machine learning models are then trained independently on each replicate and, finally, the outputs are averaged for prediction tasks or aggregated for classification tasks (for example by majority voting).

Combining bagging and causal graphical model algorithms has been proposed to improve the stability of graphical model learning [Meinshausen and Buehlmann, 2008, Li et al., 2011], as the estimation of graphical models is relatively sensitive to small changes of the original data. For example, Wang and Peng [2014] introduce an aggregation approach of directed acyclic graphs (DAGs) by minimizing the overall distance of the aggregated graph (based on structural hamming distance) to the ensemble of DAGs. In addition, the idea of measuring the uncertainty or confidence for an edge of an estimated graph from the edge frequency based on the graphs learned on bootstrap samples has been suggested in Friedman et al. [1999], Imoto et al. [2002], Mooij et al. [2016]. However, none of these approaches is directly transferable to time series causal discovery because their bootstrap sampling needs to be adapted to the lagged interdependencies of time series data.

Our **main contribution** is the introduction of a bootstrap method for time series causal discovery which preserves temporal dependencies. Our method allows (1.) to obtain **uncertainty estimates** for the links of the output graph, and (2.) **improves the stability and accuracy** by aggregating the ensemble of bootstrap graphs to one single output graph with majority voting on the level of each individual edge. In principle, our method can be paired with any time series causal discovery algorithm. Here we combine it with PCMCI+ [Runge, 2020] as a representative of a state-of-the-art constraint-based time series causal discovery method.

**The paper is structured as follows.** In Section 2, we give an overview of time series causal discovery and the PCMCI+ method. In Section 3, we present our bagging and confidence measure method which

we combine with PCMCI+ (Bagged-PCMCI+). With a range of numerical experiments, we show in Section 4 that Bagged-PCMCI+ outperforms PCMCI+ and that our method to measure confidence for links is effective. Finally, we summarize the paper in Section 5. The paper is accompanied by Supplementary Material (SM).

## 2 TIME SERIES CAUSAL DISCOVERY

### 2.1 PRELIMINARIES

We consider discrete-time structural causal processes  $\mathbf{X}_t = (X_t^1, \dots, X_t^N)$  such that

$$X_t^j := f_j(\text{pa}(X_t^j), \eta_t^j) \quad \forall j \in \{1, \dots, N\}. \quad (1)$$

Here,  $f_j$  are arbitrary measurable functions that depend non-trivially on all their arguments and  $\eta_t^j$  are mutually and temporally independent noises. In a time series graph  $\mathcal{G}$ , the nodes represent the variables  $X_t^j$  at different time lags. The *causal parents*  $\text{pa}(X_t^j)$  are the set of variables on which  $X_t^j$  depends, and a causal link from  $X_{t-\tau}^i$  to  $X_t^j$  exists if  $X_{t-\tau}^i \in \text{pa}(X_t^j)$  for a time lag  $\tau$ . A link  $X_{t-\tau}^i \rightarrow X_t^j$  is called *lagged* if  $\tau > 0$ , else it is called *contemporaneous*. In this work, we assume *stationarity* of the causal links: that is, if the causal link  $X_{t-\tau}^i \rightarrow X_t^j$  exists for some time  $t$ , then  $X_{t'-\tau}^i \rightarrow X_{t'}^j$  also exists for all times  $t' \neq t$ . We define the set  $\mathcal{A}(X_t^j)$  of non-future adjacencies of variable  $X_t^j$  as the set of all variables  $X_{t-\tau}^i$  for  $\tau \geq 0$  that have a causal link with  $X_t^j$ .

### 2.2 PCMCI+

PCMCI+ learns the causal time series graph including lagged and contemporaneous links (up to Markov equivalence) under the standard assumptions of Causal Sufficiency, Faithfulness, and the Causal Markov condition [Runge, 2020]. To increase the detection power and maintain well-calibrated tests, PCMCI+ optimizes the choice of conditioning sets in the conditional independence (CI) tests. It is based on two central ideas: (1) separating the skeleton edge removal phase into a lagged and contemporaneous conditioning phase, and (2) constructing conditioning sets in the contemporaneous conditioning phase via the so-called momentary conditional independence (MCI) approach [Runge et al., 2019c], as explained below. Moreover, PCMCI+ is order-independent [Colombo and Maathuis, 2014], which implies that the output does not depend on the order of the variables  $X^j$ . More details and examples of PCMCI+ can be found in Runge [2020], here we briefly summarize it.

In its **first phase**, PCMCI+ starts with a fully connected graph and then removes adjacencies among variable pairs by conditional independence testing. In the first phase ( $\text{PC}_1$ ), the algorithm tests all lagged pairs  $(X_{t-\tau}^i, X_t^j)$  for  $\tau > 0$  conditioning on subsets  $\mathbf{S}_k \subseteq \mathcal{A}(X_t^j) \cap \mathbf{X}_t^-$  with the lagged variables  $\mathbf{X}_t^- = (\mathbf{X}_{t-1}, \mathbf{X}_{t-2}, \dots, \mathbf{X}_{t-\tau_{\max}})$  up to a maximum time lag  $\tau_{\max}$ . If (conditional) independence is detected, the adjacency is removed. The subsets  $\mathbf{S}_k$  are chosen with increasing cardinality  $k$ : For  $k = 0$  all  $X_{t-\tau}^i$  with  $X_{t-\tau}^i \perp\!\!\!\perp X_t^j$  are removed, for  $k = 1$  those with  $X_{t-\tau}^i \perp\!\!\!\perp X_t^j | \mathbf{S}_1$  where  $\mathbf{S}_1$  is the adjacency with largest association from the previous step, for  $k = 2$  those with  $X_{t-\tau}^i \perp\!\!\!\perp Y_t | \mathbf{S}_2$  where  $\mathbf{S}_2$  are the two adjacencies with largest association from the previous step, and so on. Association strength is measured by the absolute test statistic value of the CI test. This choice improves recall and speeds up the skeleton phase. The resulting lagged adjacency sets for each  $X_t^j$  of this first phase are denoted  $\mathcal{B}_t^-(X_t^j)$ . In its **second phase**, the graph  $\mathcal{G}$  is initialized with all contemporaneous adjacencies plus all lagged adjacencies from  $\mathcal{B}_t^-(X_t^j)$  for all  $X_t^j$ . This phase of PCMCI+ tests all, contemporaneous and lagged, adjacent pairs  $(X_{t-\tau}^i, X_t^j)$  for  $\tau \geq 0$ , but iterates only through contemporaneous conditions  $\mathbf{S} \subseteq \mathcal{A}(X_t^j) \cap \mathbf{X}_t$  with the MCI test  $X_{t-\tau}^i \perp\!\!\!\perp X_t^j | \mathbf{S}, \hat{\mathcal{B}}_t^-(X_t^j) \setminus \{X_{t-\tau}^i\}, \hat{\mathcal{B}}_t^-(X_{t-\tau}^i)$ . The conditioning on  $\hat{\mathcal{B}}_t^-(X_t^j)$  blocks paths through lagged parents while the conditioning on  $\hat{\mathcal{B}}_t^-(X_{t-\tau}^i)$  has been shown to lead to well-calibrated tests even for highly autocorrelated time series [Runge et al., 2019c, Runge, 2020]. After these tests, the time-series-adapted collider orientation phase and rule orientation phase are applied: the former rule orients the collider motifs that contain contemporaneous links based on unshielded triples while the latter rule orients the remaining contemporaneous links based on the Meek rules [Meek, 1995].

In the final graph, a pair  $(X_{t-\tau}^i, X_t^j)$  of vertices can be connected by the following link types: no link (i.e., pair is non-adjacent), direct link  $X_{t-\tau}^i \rightarrow X_t^j$ , opposite direct link  $X_{t-\tau}^i \leftarrow X_t^j$  (only for  $\tau = 0$ ), unoriented link  $X_{t-\tau}^i \circ - \circ X_t^j$  (only for  $\tau = 0$ ), conflict-indicating link  $X_{t-\tau}^i \times - \times X_t^j$  (due to finite sample effects or violations of assumptions, only for  $\tau = 0$ ).

Like other CI-based methods, PCMCI+ has the free parameters  $\alpha_{PC}$  (significance level of CI tests),  $\tau_{\max}$  (maximal considered time lag), and the choice of the CI test.  $\alpha_{PC}$  in PCMCI+ has been empirically shown to be an upper bound on the false positives. As opposed to such a statistically-motivated choice, it can also be chosen based on cross-validation or an information criterion [Runge, 2020].  $\tau_{\max}$  should be larger or equal to the maximum assumed true time lag of any parent and can in practice also be chosen based on model selection. However, the numerical experiments indicate that a too large  $\tau_{\max}$  does not degrade performance much [Runge, 2020]. PCMCI+ can flexibly be combined with different CI tests for nonlinear causal discovery, and for different variable types (discrete or continuous, univariate or multivariate).

### 3 BAGGING FOR TIME SERIES CAUSAL DISCOVERY

#### 3.1 MOTIVATIONAL EXAMPLE

The example in **Fig. 1** illustrates the key benefits of bagging a causal discovery method. In this example, we generated four time series according to Equation 1 and plot them in **Fig. 1A**. We then estimate the causal dependencies from the data, once with PCMCI+ and once with Bagged-PCMCI+. In the output graph of PCMCI+, see **Fig. 1E**, it is not easily possible to assess the confidence associated with a link. Approaches in this direction are based on taking the absolute p-value over all conditioning sets [Strobl et al., 2016], which presents an overly conservative option and does not allow us to assess the confidence in orientations. In comparison, Bagged-PCMCI+ provides a measure of confidence here shown by the width of the links in **Fig. 1C** (thick links for high confidence degrees, thin links for low confidence degrees). Moreover, in this example, Bagged-PCMCI+ has fewer false positives compared to PCMCI+, which leads to higher precision and is a robust property as demonstrated by our extensive numerical experiments.

#### 3.2 BAGGED-PCMCI+

While our bootstrap approach can be adapted to any time series causal discovery algorithm, this paper focuses on its implementation with PCMCI+ called *Bagged-PCMCI+*. We illustrate the different bootstrap aggregation phases in **Fig. 1A, B and C**. The **returned results** of Bagged-PCMCI+ are: (i) an ensemble of  $B$  causal graphs from applying PCMCI+ to  $B$  datasets that are obtained by resampling with replacement while preserving temporal dependencies, (ii) the aggregation of all these graphs by majority voting (at the level of each individual edge) to a final output graph, (iii) link frequencies for the final aggregated graph that provide a confidence measure for the links.

Since time series causal discovery is sensitive to temporal dependencies, it is essential to **retain the temporal dependencies in the resampling procedure**. However, standard resampling inevitably destroys (at least parts of) the temporal dependencies. To resolve this problem, we employ the resampling strategy as illustrated in Figure 2: First, starting from the original time series  $(\mathbf{X})_{t=1}^T = (X^1, \dots, X^N)_{t=1}^T$ , we replace each component  $(X^i)_{t=1}^T$  by the  $2\tau_{\max} + 1$  dimensional vector  $(X^{*,i})_{t=2\tau_{\max}+1}^T = (X^{*,i,0}, X^{*,i,1}, \dots, X^{*,i,2\tau_{\max}})_{t=2\tau_{\max}+1}^T$ , where  $X^{*,i,\tau} = X_{t-\tau}^i$ , and define  $(\mathbf{X}^*)_{t=2\tau_{\max}+1}^T = (X^{*,1}, \dots, X^{*,N})_{t=2\tau_{\max}+1}^T$ . Second, we use standard resampling on the artificially enlarged time series  $(\mathbf{X}^*)_{t=2\tau_{\max}+1}^T$  to create the  $B$  bootstrap datasets. This procedure retains the temporal dependencies  $\mathbf{X}$  up to time lags of  $2\tau_{\max}$  because these dependencies are encoded within each *single* time step of  $\mathbf{X}^*$  by means of the auxiliary components  $X^{*,i,\tau}$ . When combined with PCMCI+ with a maximum time lag  $\tau_{\max}$ , retaining time lags up to  $2\tau_{\max}$  allows PCMCI+ to run all its CI tests; when instead combined with other causal discovery algorithms minor modifications in the definition of  $\mathbf{X}^*$  might be necessary. Moreover, we note that in our implementation the enlarged time series  $\mathbf{X}^*$  is not actually created in the sense of allocating additional memory, but instead, we employ pointers to implement the above sampling procedure. Bagged-PCMCI+ then individually applies PCMCI+ to each of the  $B$  bootstrap datasets, thus generating an ensemble  $\mathcal{C} = \{\mathcal{G}_1, \dots, \mathcal{G}_B\}$  of  $B$  causal graphs as an intermediate results. **Alg. 1** summarizes all steps up to this point.

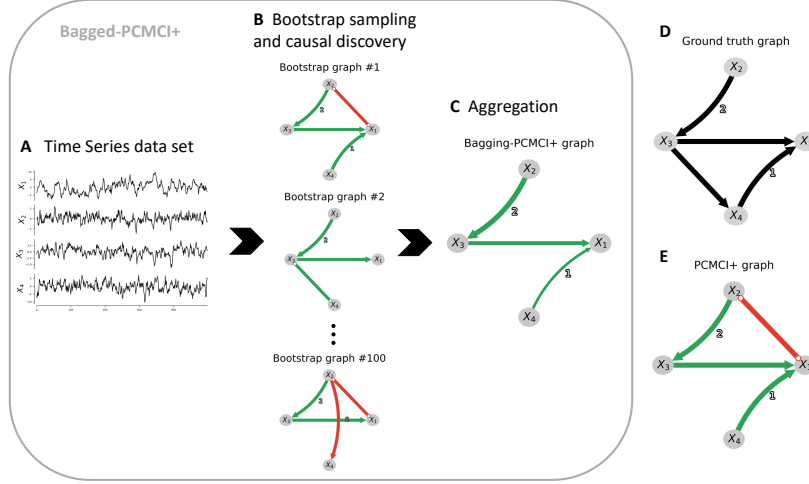


Figure 1: Motivational example and schematic of the approach. (A) Time series for a linear example of the model described in equation 1 with ground truth graph shown in (D) including the non-zero time lags as link labels. (B) 100 bootstrap replicates are generated and PCMCI+ is run independently on each of them yielding 100 bootstrap graphs. (C) The 100 graphs are aggregated to the output graph of Bagged-PCMCI+ by an edge-level majority vote. The width of the arrows of Bagged-PCMCI+ indicates a degree of confidence for a link (thick arrows for high confidence degrees, thin arrows for low confidence degrees). (E) shows the output of PCMCI+ with the original time series data. On the estimated graphs, green arrows indicate true positives. Red arrows represent false positives.

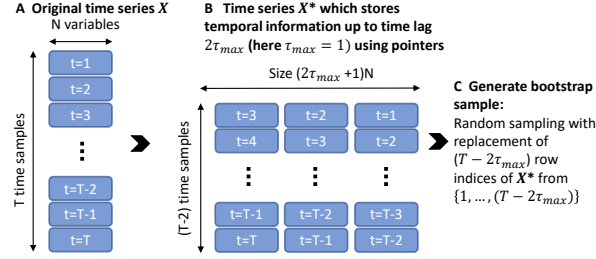


Figure 2: Bootstrap sampling scheme for time series data that retains temporal dependencies up to a maximum time lag  $2\tau_{\max}$  (here  $\tau_{\max} = 1$ ). (A) Original time series  $\mathbf{X}$ . (B) Extended time series  $\mathbf{X}^*$  that encodes temporal dependencies up to  $2\tau_{\max}$ , see explanation in the text (C) Bootstrap replicates: a standard bootstrap sampling of the time indices can be carried out on  $\mathbf{X}^*$ .

---

**Algorithm 1:** (Bootstrap sampling procedure and creation of bootstrap causal graphs )

---

**input** : Number of bootstrap realizations  $B$ , dataset  $\mathbf{X} = (X_1, \dots, X_T) \in \mathbb{R}^{(T \times N)}$ , a causal discovery algorithm (for example PCMCI+), maximum time lag  $\tau_{\max}$

**output** : Ensemble of bootstrap causal graphs  $\mathcal{C} = (\mathcal{G}_1, \dots, \mathcal{G}_B)$

Initialize enlarged time series dataset  $(\mathbf{X}^*)_{t=2\tau_{\max}+1}^T$  as explained in the text (also see Fig. 2);

**for**  $b = 1$  **to**  $B$  **do**

    Seed  $S \leftarrow$  New and unique seed for iteration  $b$ ;

    Indices  $I_b \leftarrow \{\text{Set of } (T - 2\tau_{\max}) \text{ integers randomly sampled from } [2\tau_{\max}, T] \text{ with replacement using the random seed } S\}$ ;

    /\* Resampled time series  $\mathbf{X}_b^*$  with the time indices  $I_b$  of  $\mathbf{X}^*$  : \*/

$\mathbf{X}_b^* \leftarrow \mathbf{X}^*[I_b, \dots]$ ;

    /\* Run causal discovery algorithm with dataframe  $\mathbf{X}_b^*$  \*/

$\mathcal{G}_b \leftarrow$  Output of time series causal discovery algorithm with input  $\mathbf{X}_b^*$ ;

**end**

**return**  $\mathcal{C} = \{\mathcal{G}_1, \dots, \mathcal{G}_B\}$

---

In **Alg. 2**, we detail the aggregation of the  $B$  causal graphs  $\mathcal{C} = \{\mathcal{G}_1, \dots, \mathcal{G}_B\}$  to a single final output graph  $\mathcal{G}_{bagged}$  and the quantification of confidences. For each pair of vertices  $(X_{t-\tau}^i, X_t^j)$  we iterate through the graphs  $\mathcal{G}_1, \dots, \mathcal{G}_B$  and record the relative frequency of each of the possible link types. The possible link types are: no link,  $\rightarrow$ ,  $\leftarrow$ ,  $\circ-\circ$ ,  $\times-\times$  (the last three only for  $\tau = 0$ ). For **aggregation**, different strategies are possible. Here, we aggregate by relative majority voting of the link types for each pair  $(X_{t-\tau}^i, X_t^j)$  individually. Ties are resolved by the preference order no link,  $\times-\times$  and  $\circ-\circ$ ; and in case of a tie between  $\rightarrow$  and  $\leftarrow$  a conflicting link  $\times-\times$  is returned. One benefit of aggregating at the level of individual edges is simplicity. However, it can result in cyclic aggregated graphs, which might not be desirable. The exploration of alternative aggregation methods, e.g. by adapting current techniques that minimize a modified structural Hamming distance of the aggregated graph to the entire set of graphs [Wang and Peng, 2014], can be considered in future research. To quantify **confidences**, we employ the relative frequencies of link types. For example, if a link in  $\mathcal{G}_{bagged}$  occurs in 80% of the ensemble graphs in  $\mathcal{C}$ , then we have stronger confidence in this link than in a different link in  $\mathcal{G}_{bagged}$  that occurs only in 45% of the ensemble graphs.

---

**Algorithm 2:** (Aggregation of bootstrap causal graphs by majority voting of edges)

---

**input** : Ensemble of bootstrap causal graphs  $\mathcal{C} = \{\mathcal{G}_1, \dots, \mathcal{G}_B\}$

**output** : Aggregated graph  $\mathcal{G}_{bagged}$ , the relative frequency  $F$  of link types for each pair of vertices  $(X_{t-\tau}^i, X_t^j)$  and link type  $e$  across  $\mathcal{C}$

Initialize an empty graph  $\mathcal{G}_{bagged}$  with the same nodes as in the bootstrap causal graphs;  
Initialize a two-level nested dictionary  $F$  for recording relative frequencies of link types;

**forall** pairs  $(X_{t-\tau}^i, X_t^j)$  with  $0 \leq \tau \leq \tau_{\max}$ ,  $1 \leq i, j \leq N$ , and  $i < j$  if  $\tau = 0$  **do**

**forall** possible link types  $e$  **do**

$n(e) \leftarrow$  number of graphs in  $\mathcal{C}$  in which  $(X_{t-\tau}^i, X_t^j)$  is connected by  $e$  ;

$F[(X_{t-\tau}^i, X_t^j)][e] \leftarrow \frac{n(e)}{B}$ ;

**end**

    /\* Majority vote of link types:

\*/

    Link between  $(X_{t-\tau}^i, X_t^j)$  in  $\mathcal{G}_{bagged} \leftarrow \operatorname{argmax}_e F[(X_{t-\tau}^i, X_t^j)][e]$ ;

**end**

**return**  $\mathcal{G}_{bagged}, F$

---

### 3.3 THEORETICAL RESULTS

Based on the results of numerical experiments and the asymptotic consistency of PCMCi+, we conjecture that Bagged-PCMCi+ is asymptotically consistent in the following sense.

**Assumption 1** *We assume Causal Sufficiency, the Causal Markov Condition, the Faithfulness Conditions, and consistent CI tests (oracle). We also assume stationarity, time-order, and that the maximum time lag  $\tau_{\max} \geq \tau_{\max}^{\text{pa}}$ , where  $\tau_{\max}^{\text{pa}}$  is the maximum time lag of any parent in the model 1. We rule out selection variables and measurement errors.*

**Conjecture 1 (Asymptotic consistency)** *Under Assumptions 1 and as the number  $T$  of time steps goes to infinity, Bagged-PCMCi+ returns the correct partially directed acyclic graph (CPDAG), i.e., the graph with correct adjacencies and links oriented as much as possible.*

We provide more details in the SM. What we are not yet able to prove is that the CI tests remain consistent when they are applied to the resampled datasets rather than the original dataset.

## 4 NUMERICAL EXPERIMENTS

### 4.1 BAGGED-PCMCi+ EVALUATION ON SYNTHETIC DATA

The numerical experiments model a number of typical challenges in time series causal discovery [Runge et al., 2019a]: contemporaneous and time lagged causal dependencies, strong autocorrelation, large numbers of variables and considered time lags. For better comparison to PCMCi+, we

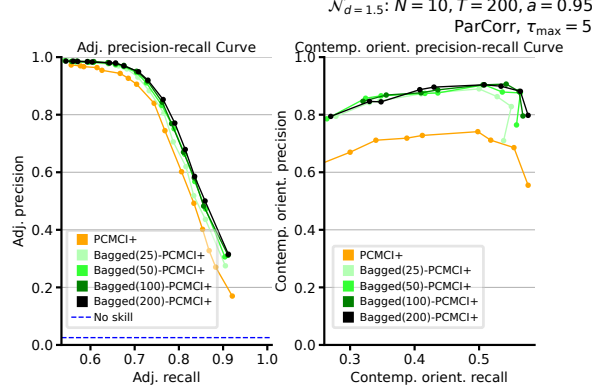


Figure 3: Precision-recall curves for adjacencies (left) and contemporaneous orientations (right) obtained by varying the significance level  $\alpha_{PC}$  in PCMCI+ and Bagged-PCMCI+ for the model setup as shown in top right. Results are shown for PCMCI+ (orange line) and Bagged-PCMCI+ with different numbers of bootstrap replicas  $B$  (lines with different shades of green).

use a similar setup to the numerical experiments presented in Runge [2020]. The synthetic data is generated according to the following additive model:

$$X_t^j = a_j X_{t-1}^j + \sum_i f_i(X_{t-\tau_i}^i) + \eta_t^j \quad \forall j \in \{1, \dots, N\} \quad (2)$$

Autocorrelation coefficients  $a_j$  are uniformly drawn from  $[\max(0, a - 0.3), a]$  for  $a$  as indicated in the header of the corresponding figures. The noise terms  $\eta_j$  are independent and identically distributed zero-mean Gaussians  $\mathcal{N}(0, \sigma^2)$  with standard deviation  $\sigma$  drawn from  $[0.5, 2]$ . In addition to autodependency links, for each model  $L = \lfloor 1.5 \cdot N \rfloor$  (for  $N = 2$ ,  $L = 1$ ) cross-links are chosen with linear functional dependencies  $f_i(x) = x$ . Coefficients  $c_i$  are drawn uniformly from  $\pm[0.1, 0.5]$ . 30% of the links are contemporaneous ( $\tau_i = 0$ ) and the remaining 70% are lagged links with  $\tau_i$  drawn from  $\{1, \dots, 5\}$ . Only stationary models are considered. We have an average cross-in-degree of  $d = 1.5$  for all network sizes (plus an auto-dependency) implying that models become sparser for larger  $N$ . We consider the PCMCI+ algorithm and Bagged( $B$ )-PCMCI+ where  $B$  is the number of bootstrap realizations (here 25, 50, 100, and 200). Both algorithms use partial correlation (ParCorr) for the conditional independence tests.

Performance is evaluated with recall (equivalent to True Positive Rate, TPR) and precision. For adjacencies, precision and recall are distinguished between lagged cross-links ( $i \neq j$ ), contemporaneous ( $\tau = 0$ ), and autodependency links ( $i = j$ ). Due to time order, lagged links (and autodependencies) are automatically oriented. Performance of contemporaneous orientation is evaluated with contemporaneous orientation precision which is measured as the fraction of correctly oriented links ( $\circ \rightarrow \circ, \rightarrow, \leftarrow$ ) among all estimated adjacencies, and with recall as the fraction of correct orientations among all true contemporaneous links. False positive rates (FPR) are also shown to evaluate whether the methods control false positives at the chosen significance level  $\alpha_{PC}$ . In addition,  $F_1$  scores are calculated for adjacencies and contemporaneous orientations as the harmonic mean of precision and recall:  $F_1 = 2 \frac{\text{precision} \cdot \text{recall}}{\text{precision} + \text{recall}}$ . Furthermore, the fraction of conflicting links among all detected contemporaneous adjacencies is calculated. Finally, we give the average runtimes that were evaluated on an AMD EPYC 7763 processor. All metrics (and their standard errors) are computed across all estimated graphs from 500 different additive models (and associated realizations) described in 2 with time series length  $T$ .

**Figure 3** depicts **precision-recall curves** for adjacencies as well as contemporaneous orientations obtained by varying the hyperparameter  $\alpha_{PC}$  for a model setup that stands exemplary for others (see SM). The precision-recall values of Bagged-PCMCI+ are systematically higher than those of PCMCI+, regarding adjacencies and even more pronounced for contemporaneous orientations. Moreover, larger numbers of bootstrap replicates  $B$  results in enhanced performance, but we observe no strong differences between  $B = 50$  and  $B = 200$ . More precision-recall curves are shown in the SM for different model parameters (autocorrelation, number of variables, and time sample size).

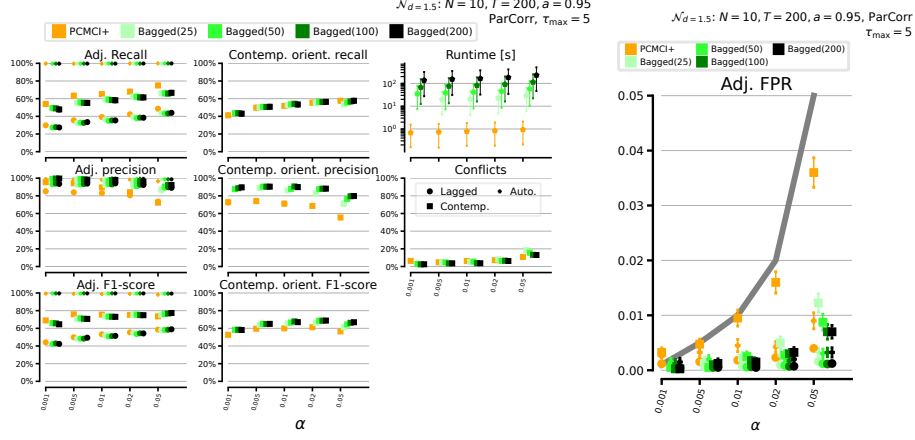


Figure 4: Numerical experiments with linear Gaussian setup for varying significance level  $\alpha_{PC}$  of PCMCI+.

Noticeably, we found that Bagged-PCMCI+ outperforms PCMCI+ more clearly in statistically more challenging regimes with higher autocorrelation  $a$ , larger number of variables  $N$ , and smaller time sample sizes  $T$ .

**Figure 4** depicts further details for the linear Gaussian setup for varying significance level  $\alpha_{PC}$  with model parameters shown at the top right. The right column of **Fig. 4** clearly shows that both methods (PCMCI+ and Bagged-PCMCI+) control the FPR below the significance level  $\alpha_{PC}$  (grey line), but Bagged-PCMCI+ consistently exhibits **lower FPR** compared to PCMCI+ for all types of links (lagged, contemporaneous, and all) and across significance levels  $\alpha_{PC}$  ranging from 0.001 to 0.1. Thus, treating the significance level as a hyperparameter, one can use a much higher level  $\alpha_{PC}$  for Bagged-PCMCI+ than for PCMCI+ while still controlling the FPR below  $\alpha_{PC}$ .

The adjacency results (left-most column of Fig. 4) for different  $\alpha_{PC}$  show higher precision of Bagged-PCMCI+ over PCMCI+, but also slightly lower recall – at a given  $\alpha_{PC}$ . The aggregate measure F1 then is similar or larger for Bagged-PCMCI+.

For contemporaneous orientation recall the performance gain is even more evident with stronger improvement in precision and smaller improvements in recall.

There appear to be slightly fewer conflicts for Bagged-PCMCI+. Runtimes are, as expected, higher for Bagged-PCMCI+, but these can be reduced by embarrassingly parallelization.

In SM, we provide additional figures for varying one of autocorrelation  $a$ , number of variables  $N$ , time sample size  $T$ , and maximum time lag  $\tau_{\max}$  with  $\alpha_{PC} = 0.01$ . We found that Bagged-PCMCI+ seem robust to large maximum time lags  $\tau_{\max}$  (even when  $\tau_{\max}$  is much larger than the true maximum time lag of 5) for the studied sample size  $T = 500$ .

We have also combined our bagging approach with a modified PC algorithm adapted to time series. We provide results for this experiment in SM. Similar to PCMCI+, we have found that Bagged-PC enhances its base algorithm PC in terms of precision and recall.

## 4.2 EVALUATION OF BAGGED-PCMCI+ CONFIDENCE MEASURE

We conduct numerical experiments to assess the ability of Bagged-PCMCI+ to determine a confidence degree for links in the output graph. It is essential to have a reference point for comparing our proposed confidence measure. Ideally, we would like the Bagged-PCMCI+ link frequency obtained on a single data sample to approximate closely the frequency of links along graphs obtained independently by PCMCI+ on an infinite number of data samples, which we call true link frequencies. In practice, it is only possible to approximate the true link frequencies by using a large but limited number of data samples. Here, we design two experiments to evaluate the ability of the proposed confidence measures to approximate the true link frequencies.



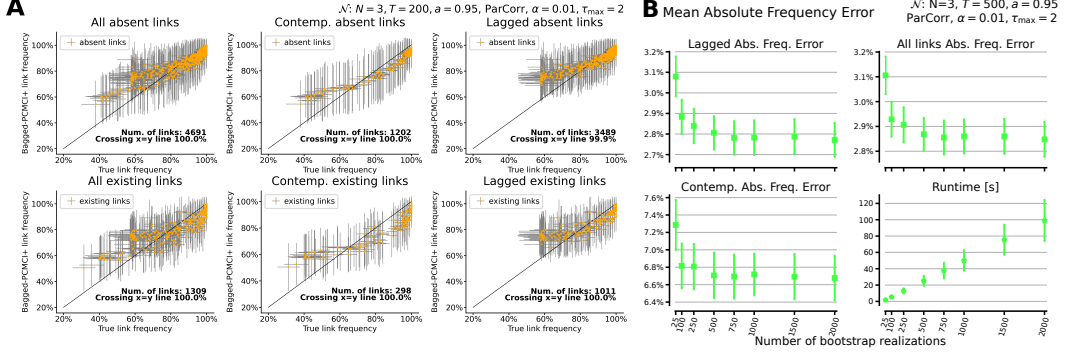


Figure 5: (A) Estimated true link frequencies against mean Bagged-PCMCI+ link frequencies ( $B = 1000$ ) for a linear Gaussian setup with parameters indicated at the top right. Grey bars indicate the one-standard-deviation error bars around the estimated value. (B) Mean absolute frequency error between estimated true link frequencies and Bagged-PCMCI+ link frequencies for varying  $B$  and a linear Gaussian setup with parameters indicated at the top right.

In the **first experiment**, we generate 100 different additive models (see equation 2). For each of these models, we generate  $D = 500$  independent data samples with the same additive model (only the noise terms change across the samples). For each of the 500 samples, causal graphs are estimated independently using PCMCI+ and Bagged-PCMCI+. For each edge, we estimate its true link frequency by calculating the frequency of the most recurrent link types across the PCMCI+ ensemble of 500 graphs. We use the mean of our proposed confidence measure (i.e. the mean of the Bagged-PCMCI+ link frequencies along the 500 Bagged-PCMCI+ graphs) to reduce the amount of noise in the estimation. We also calculate the standard deviation of the Bagged-PCMCI+ link frequency along the 500 Bagged-PCMCI+ graphs to estimate its uncertainty. If effective, we expect the Bagged-PCMCI+ confidence measure to approximately follow the estimated true link frequency.

In Fig. 5A, we show the results of the latter experiment for model parameters and method parameters shown at the top right and for  $B = 1000$ . We plot confidence measures against the true link frequencies for different causal dependencies (lagged, contemporaneous, or all) and for existing/absent links of the ground truth graphs. Figure 5A shows that the Bagged-PCMCI+ link frequency (confidence measure) follows the true link frequency. We can notice a bias for low true link frequencies as Bagged-PCMCI+ tends to overestimate the true link frequencies between 40% to 60%. This bias seems consistent across different types of causal dependencies. It is still visible when varying the number of bootstrap realizations  $B$  as shown in SM. The one-standard-deviation error bars give indications of the uncertainties in the confidence measure and the estimated true link frequency. When taking into account both uncertainties, the error bars cross the expected  $x = y$  diagonal line more than 99% of the estimated link frequencies. This high percentage demonstrates that the Bagged-PCMCI+ confidence measure approximates the true link frequency of PCMCI+.

In the **second experiment**, we quantify the average absolute error of the Bagged-PCMCI+ link frequency relative to the True Link Frequency for different causal dependencies (lagged, contemporaneous, or all) and for existing links and absent links of the ground truth model. For one additive model, the true link frequency is calculated as the frequency of the most recurrent link type of PCMCI+ graphs over  $D = 5000$  independent samples. Here the Bagged-PCMCI+ link frequency is a confidence measure for the first data sample for this additive model. We calculate the mean absolute error between the confidence measures and the estimated true link frequencies. We generate a total of 500 different additive models and average the mean absolute link frequency errors. To study the effect of the number of bootstrap realizations  $B$  on the error, we vary  $B$  from 25 to 2000.

We present the results of the mean absolute link frequency errors in Fig 5B. For lagged links, auto links, and all links, the mean absolute errors are a bit higher than 3% which seems relatively low. For the contemporaneous links, the 7% errors demonstrate that the estimation of the contemporaneous links is a more difficult task for the current method. It is also yet not clear if the mean absolute error converges to zero if  $B$  goes to infinity. We observe that a larger  $B$  leads to a lower mean absolute error of Bagged-PCMCI+. This confirms that increasing  $B$  enhances the performance of the Bagged-PCMCI+. The mean absolute frequency error reduces by about 10% when increasing  $B$

from 25 to 500. Unfortunately, the increase in performance comes at the cost of a 20-fold increase in runtime. This is why we recommend using a number of bootstrap realizations which is adapted for the application and available computing resources, but preferably larger or equal to 100.

## 5 CONCLUSION

In this paper, we have made **two major contributions** to time series causal discovery. First, we propose a **bootstrap aggregation** by majority voting that can be combined with any time series causal discovery algorithm. Here, we combine our bootstrap aggregation approach with the state-of-the-art time series causal discovery PCMCI+ algorithm (referred to as Bagged-PCMCI+). Through extensive numerical experiments, we show that Bagged-PCMCI+ greatly reduces the number of false positives compared to the base PCMCI+ algorithm. In addition, Bagged-PCMCI+ has a higher precision-recall regarding adjacencies and orientations of contemporaneous edges compared to PCMCI+. Our second contribution is a **confidence measure for links** in a time series graph, which is calculated as the link frequencies along the graphs learned on bootstrap replicates. Numerical experiments show that the proposed method gives a pertinent confidence measure for links of the output graph. The **main strengths** of our method is that it can be coupled with any time series causal discovery algorithm, and it can be of substantial use in many real-world applications, especially for orienting contemporaneous causal links or when confidence measures for links are desired. The **main weaknesses** of our method so far are its higher computational cost and longer runtime. One solution to decrease runtime is to parallelize the bootstrap process. In addition, the current method of aggregating through majority voting has a limitation. It can lead to cyclic graphs that are not always desirable. Therefore, exploring alternative methods of aggregation will constitute a crucial step for future research. The topic of causal discovery is fundamental, and we believe **the risk of misuse** is low.

## Acknowledgements

K.D. and V.E. received funding from the European Research Council (ERC) Synergy Grant “Understanding and modeling the Earth System with Machine Learning (USMILE)” under the European Union’s Horizon 2020 research and innovation programme (Grant agreement No. 855187). J.R. received funding from the ERC Starting Grant CausalEarth under the European Union’s Horizon 2020 research and innovation program (Grant Agreement No. 948112). This work used resources of the Deutsches Klimarechenzentrum (DKRZ) granted by its Scientific Steering Committee (WLA) under project ID 1083. We thank Birgit Kühbacher for her insightful comments that helped improve the paper. We also thank Tom Hochsprung for his remarks and our fruitful discussions.

## References

- L. Breiman. Bagging predictors. *Machine Learning*, 24:123–140, 1996.
- David Maxwell Chickering. Learning equivalence classes of bayesian-network structures. *J. Mach. Learn. Res.*, 2:445–498, 1996.
- Diego Colombo and Marloes H. Maathuis. Order-independent constraint-based causal structure learning. *J. Mach. Learn. Res.*, 15(1):3741–3782, jan 2014. ISSN 1532-4435.
- Nir Friedman, Moisés Goldszmidt, and Abraham J. Wyner. Data analysis with bayesian networks: A bootstrap approach. *ArXiv*, abs/1301.6695, 1999.
- Nir Friedman, Michal Linial, Iftach Nachman, and Dana Pe’er. Using bayesian networks to analyze expression data. In *Annual International Conference on Research in Computational Molecular Biology*, 2000.
- Evgenia Galytska, Katja Weigel, Dörthe Handorf, Ralf Jaiser, Raphael Harry Köhler, Jakob Runge, and Veronika Eyring. Causal model evaluation of arctic-midlatitude teleconnections in CMIP6. 2022 (in review). doi: 10.1002/essoar.10512569.1.
- Andreas Gerhardus and Jakob Runge. High-recall causal discovery for autocorrelated time series with latent confounders. In H. Larochelle, M. Ranzato, R. Hadsell, M.F. Balcan, and H. Lin, editors, *Advances in Neural Information Processing Systems*, volume 33, pages 12615–12625. Curran Associates, Inc., 2020.
- Clive W. J. Granger. *Investigating Causal Relations by Econometric Models and Cross-Spectral Methods*, volume 2 of *Econometric Society Monographs*, page 31–47. Cambridge University Press, 2001. doi: 10.1017/CBO9780511753978.002.
- Aapo Hyvärinen, Kun Zhang, Shohei Shimizu, and Patrik O. Hoyer. Estimation of a structural vector autoregression model using non-gaussianity. *Journal of Machine Learning Research*, 11(56): 1709–1731, 2010.
- Guido W. Imbens and Donald B. Rubin. *Causal Inference for Statistics, Social, and Biomedical Sciences: An Introduction*. Cambridge University Press, 2015. doi: 10.1017/CBO9781139025751.
- Seiya Imoto, Sun Yong Kim, Hidetoshi Shimodaira, Sachiyo Aburatani, Kousuke Tashiro, Satoru Kuhara, and Satoru Miyano. Bootstrap analysis of gene networks based on bayesian networks and nonparametric regression. *Genome Informatics*, 13:369–370, 2002.
- Maciej Kaminski, Mingzhou Ding, Wilson A. Truccolo, and Steven L. Bressler. Evaluating causal relations in neural systems: Granger causality, directed transfer function and statistical assessment of significance. *Biological Cybernetics*, 85:145–157, 2001.
- Soufiane Karmouche, Evgenia Galytska, Jakob Runge, Gerald A. Meehl, Adam S. Phillips, Katja Weigel, and Veronika Eyring. Regime-oriented causal model evaluation of atlantic–pacific teleconnections in cmip6. *Earth System Dynamics*, 2023.
- Shuang Li, Li Hsu, Jie Peng, and Pei Wang. Bootstrap inference for network construction with an application to a breast cancer microarray study. *The annals of applied statistics*, 7 1:391–417, 2011.
- Christopher Meek. Causal inference and causal explanation with background knowledge. In *Proceedings of the Eleventh Conference on Uncertainty in Artificial Intelligence*, UAI’95, page 403–410, San Francisco, CA, USA, 1995. Morgan Kaufmann Publishers Inc. ISBN 1558603859.
- Nicolai Meinshausen and Peter H. Bühlmann. Stability selection. *Journal of the Royal Statistical Society: Series B (Statistical Methodology)*, 72, 2008.
- Joris M. Mooij, Sara Magliacane, and Tom Claassen. Joint causal inference from multiple contexts. *J. Mach. Learn. Res.*, 21:99:1–99:108, 2016.
- Peer Johannes Nowack, Jakob Runge, Veronika Eyring, and Joanna D. Haigh. Causal networks for climate model evaluation and constrained projections. *Nature Communications*, 11, 2020.

- Judea Pearl. *Causality*. Cambridge University Press, 2 edition, 2009. doi: 10.1017/CBO9780511803161.
- Joseph Ramsey, Peter Spirtes, and Jiji Zhang. Adjacency-faithfulness and conservative causal inference. In *Proceedings of the Twenty-Second Conference on Uncertainty in Artificial Intelligence*, UAI'06, page 401–408, Arlington, Virginia, USA, 2006. AUAI Press. ISBN 0974903922.
- Donald B. Rubin. Estimating causal effects of treatments in randomized and nonrandomized studies. *Journal of Educational Psychology*, 66:688–701, 1974.
- Jakob Runge. Discovering contemporaneous and lagged causal relations in autocorrelated nonlinear time series datasets. In *Conference on Uncertainty in Artificial Intelligence*, 2020.
- Jakob Runge, Sebastian Bathiany, Erik M. Bollt, Gustau Camps-Valls, Dim Coumou, Ethan R. Deyle, Clark Glymour, Marlene Kretschmer, Miguel D. Mahecha, Jordi Muñoz-Marí, Egbert H. van Nes, J. Peters, Rick Quax, Markus Reichstein, Marten Scheffer, Bernhard Schölkopf, Peter L. Spirtes, George Sugihara, Jie Sun, Kun Zhang, and Jakob Zscheischler. Inferring causation from time series in earth system sciences. *Nature Communications*, 10, 2019a.
- Jakob Runge, Peer Nowack, Marlene Kretschmer, Seth Flaxman, and Dino Sejdinovic. Detecting and quantifying causal associations in large nonlinear time series datasets. *Science Advances*, 5 (11):eaau4996, 2019b. doi: 10.1126/sciadv.aau4996.
- Jakob Runge, Peer Nowack, Marlene Kretschmer, Seth Flaxman, and Dino Sejdinovic. Detecting and quantifying causal associations in large nonlinear time series datasets. *Science advances*, 5 (11):eaau4996, 2019c.
- Peter Spirtes, Clark Glymour, Scheines N., and Richard. *Causation, Prediction, and Search*. MIT Press: Cambridge, 2000.
- Peter L. Spirtes and Clark Glymour. An algorithm for fast recovery of sparse causal graphs. *Social Science Computer Review*, 9:62 – 72, 1991.
- Eric V. Strobl, Peter L. Spirtes, and Shyam Visweswaran. Estimating and controlling the false discovery rate of the pc algorithm using edge-specific p-values. *ACM Transactions on Intelligent Systems and Technology (TIST)*, 10:1 – 37, 2016.
- George Sugihara, Robert M. May, Hao Ye, Chih-hao Hsieh, Ethan R. Deyle, Michael Fogarty, and Stephan B. Munch. Detecting causality in complex ecosystems. *Science*, 338:496 – 500, 2012.
- Ru Wang and Jie Peng. Learning directed acyclic graphs via bootstrap aggregating. *arXiv: Machine Learning*, 2014.
- Jiji Zhang. On the completeness of orientation rules for causal discovery in the presence of latent confounders and selection bias. *Artif. Intell.*, 172:1873–1896, 2008.

## SUPPLEMENTARY MATERIAL

The Supplementary Material includes:

- Results of additional numerical experiments for our proposed approach Bagged-PCMCI+
- Results of numerical experiments for an alternative approach: Bagged-PC (bagging approach combined with the time-series adapted PC algorithm instead of PCMCI+)
- More details on our conjecture that Bagged-PCMCI+ is asymptotically consistent, as given in Section 3.3 of the main text.
- Python code to reproduce the numerical experiments in a separate github repository. Please refer to the README.md in the repository for more details.

## S1 ADDITIONAL NUMERICAL EXPERIMENTS

### S1.1 BAGGED-PCMCI+ METHOD EVALUATION

#### S1.1.1 FURTHER PRECISION-RECALL CURVES

Precision-recall curves for additional model setups show the impact of a smaller number of variables of  $N = 5$  instead of  $N = 10$  in the main text (**Fig. 6**), increased sample size  $T$  from 200 to 500 for  $N = 5$  (**Fig. 8**), and a decreased autocorrelation coefficient  $a$  from 0.95 to 0.6 for  $T = 500$  and  $N = 5$  (**Fig. 10**). For all these model setups we also provide the individual precisions, recalls, F1-scores plots for adjacencies and contemporaneous orientations, as well as the runtimes and number of conflicts for varying  $\alpha_{PC}$  (see **Figs. 7, 9, and 11**).

Across all these model setups, for a given  $\alpha_{PC}$  Bagged-PCMCI+ has similar recall and higher precision as compared to PCMCI+, particularly in orienting contemporaneous links. Moreover, these improvements are stronger in the more challenging settings (high autocorrelation  $a$ , short time sample size  $T$ , and high number of variables  $N$ ).

While, for a given  $\alpha_{PC}$ , PCMCI+ can have higher adjacency recall, the fair comparison here is the area under the precision-recall curve, which is higher for Bagged-PCMCI+. This implies that one can always choose a higher  $\alpha_{PC}$  to obtain a better recall with Bagged-PCMCI+, while still retaining the same or better precision.

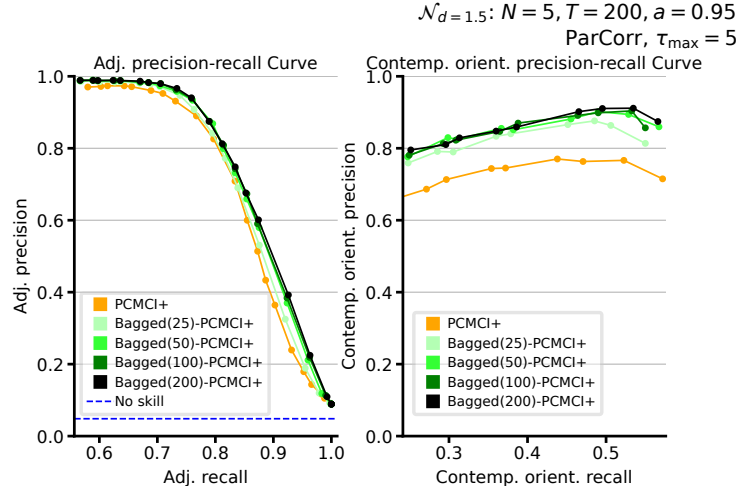


Figure 6: Precision-recall curves for adjacencies (left) and contemporaneous orientations (right) obtained by varying the significance level  $\alpha_{PC}$  in PCMCI+ and Bagged-PCMCI+ for the model setup as shown in the header. Results are for PCMCI+ (orange line) and Bagged-PCMCI+ with different numbers of bootstrap replicas  $B$  (lines with different shades of green). Here  $N = 5$ ,  $T = 200$ , and  $a = 0.95$ .

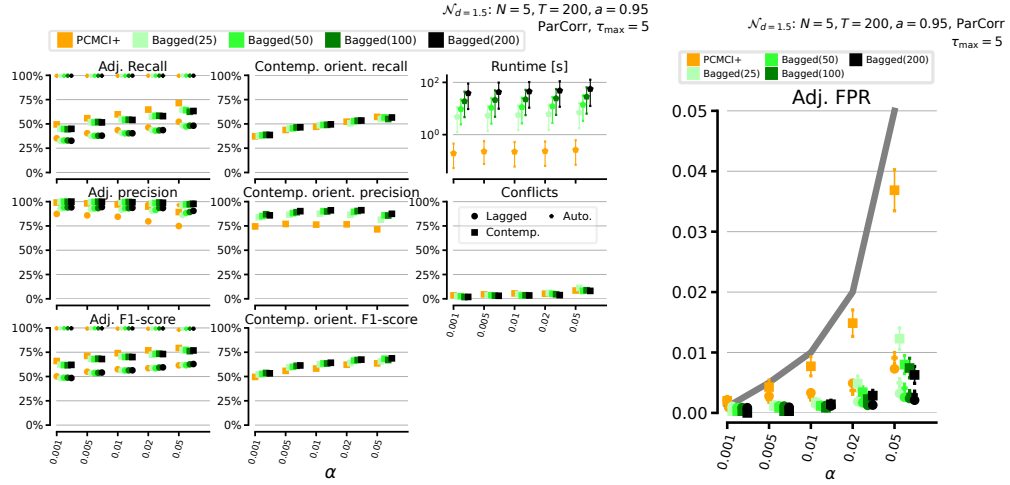


Figure 7: Numerical experiments with linear Gaussian setup for varying  $\alpha_{PC}$  of PCMCi+. Here  $N = 5$ ,  $T = 200$ , and  $a = 0.95$ .

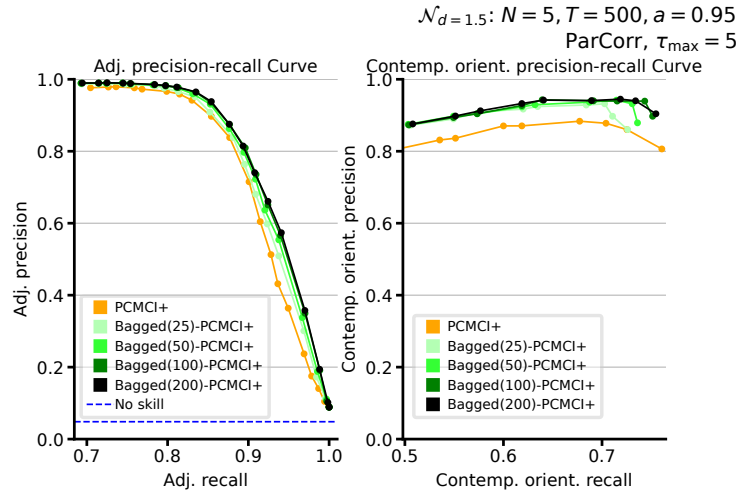


Figure 8: Precision-recall curves for adjacencies (left) and contemporaneous orientations (right) obtained by varying the significance level  $\alpha_{PC}$  in PCMCi+ and Bagged-PCMCi+ for the model setup as shown in the header. Results are for PCMCi+ (orange line) and Bagged-PCMCi+ with different numbers of bootstrap replicas  $B$  (lines with different shades of green). Here  $N = 5$ ,  $T = 500$ , and  $a = 0.95$ .

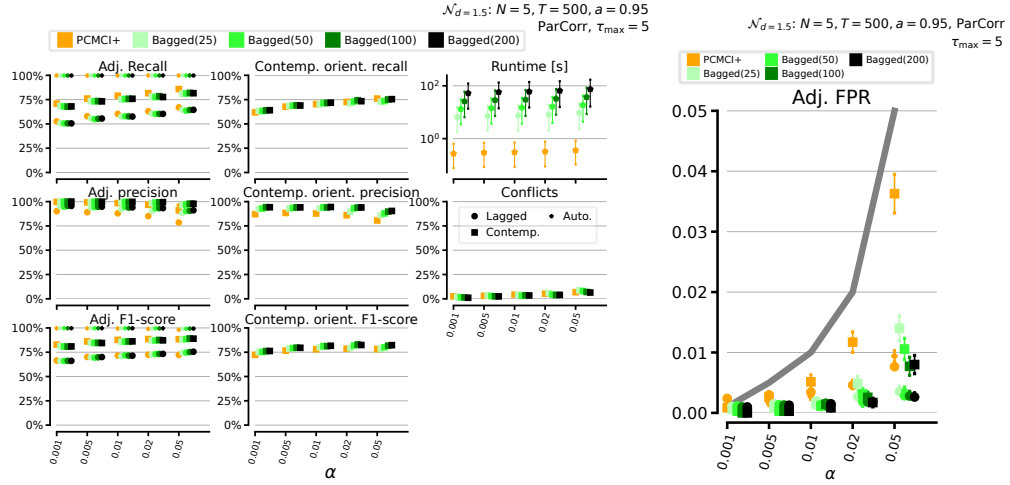


Figure 9: Numerical experiments with linear Gaussian setup for varying  $\alpha_{PC}$  of PCMCi+. Here  $N = 5$ ,  $T = 500$ , and  $a = 0.95$ .

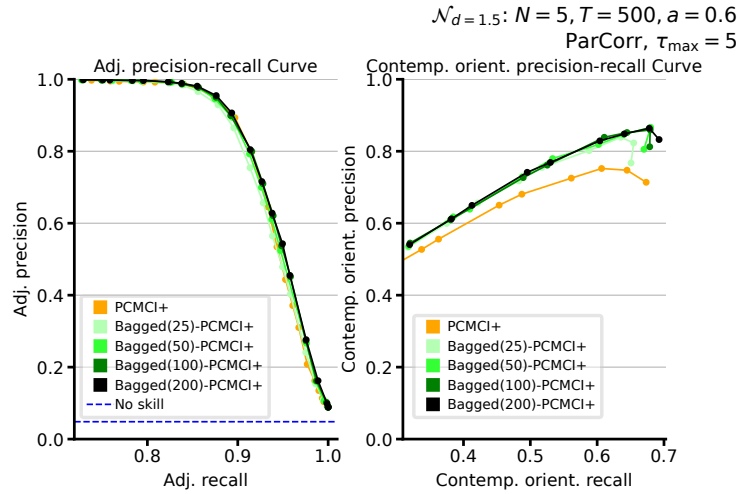


Figure 10: Precision-recall curves for adjacencies (left) and contemporaneous orientations (right) obtained by varying the significance level  $\alpha_{PC}$  in PCMCi+ and Bagged-PCMCi+ for the model setup as shown in the header. Results are for PCMCi+ (orange line) and Bagged-PCMCi+ with different numbers of bootstrap replicas  $B$  (lines with different shades of green). Here  $N = 5$ ,  $T = 500$ , and  $a = 0.6$ .

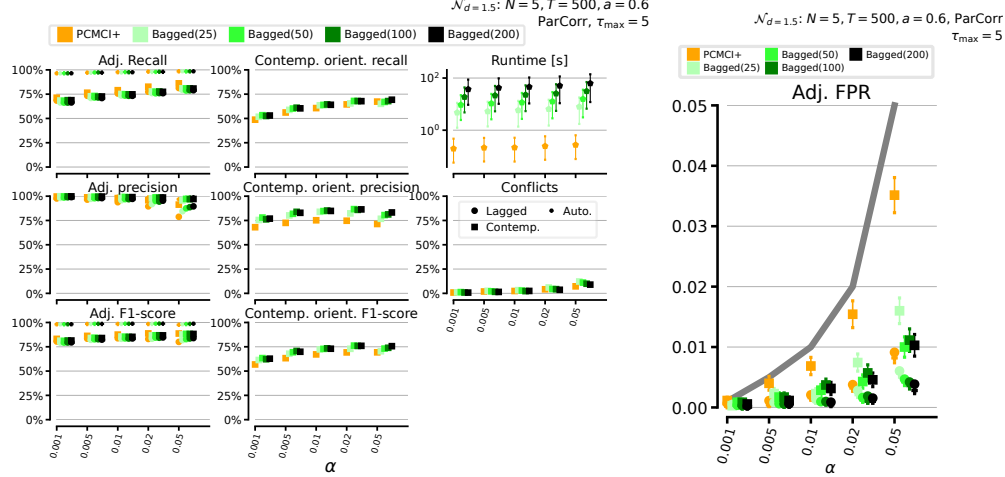


Figure 11: Numerical experiments with linear Gaussian setup for varying  $\alpha_{PC}$  of PCMCi+. Here  $N = 5$ ,  $T = 500$ , and  $a = 0.6$ .

### S1.1.2 FURTHER EXPERIMENTS

Here we study in more detail the impact of different model parameters on the performance of Bagged-PCMCi+. We vary the following model parameters: autocorrelation  $a$  (Fig. 12), number of variables  $N$  (Fig. 13), time sample size  $T$  (Fig. 14), and maximum time lag  $\tau_{\max}$  (Fig. 15) for a fixed significance level  $\alpha_{PC} = 0.01$ . The default model parameters, if not varied in the experiment, are  $a = 0.95$ ,  $T = 500$ , and  $N = 5$ .

For all setups, these numerical experiments confirm the lower FPR of Bagged-PCMCi+ over PCMCi+ for a fixed significance level  $\alpha_{PC} = 0.01$ . For increasing autocorrelation  $a$ , we observe a slight gain in the orientation F1-score of Bagged-PCMCi+ over PCMCi+. For small sample size  $T$ , PCMCi+ has very slightly higher adjacency F1-scores, but lower orientation F1-score. For increasing number of variables  $N$  we observe the largest gains in both adjacency and orientation F1-scores for Bagged-PCMCi+ over PCMCi+. There is almost no change in both Bagged-PCMCi+ and PCMCi+ for increasing the maximum time lag  $\tau_{\max}$ , illustrating the robustness of these methods to this hyperparameter.

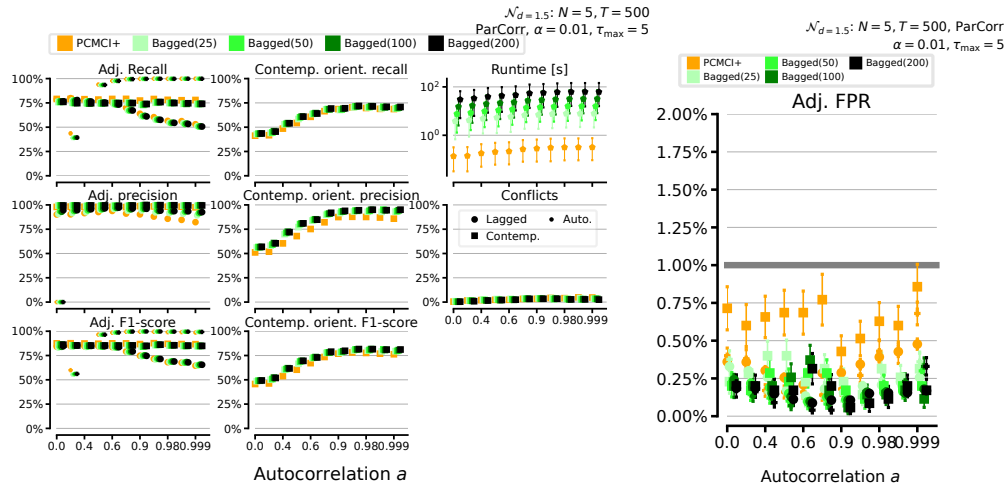


Figure 12: Numerical experiments with linear Gaussian setup for a varying autocorrelation.



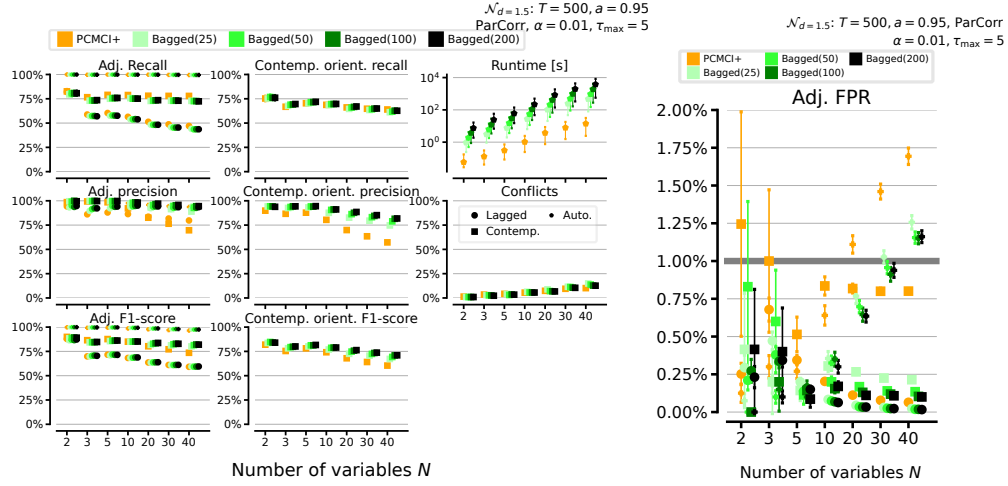


Figure 13: Numerical experiments with linear Gaussian setup for a varying number of variables.

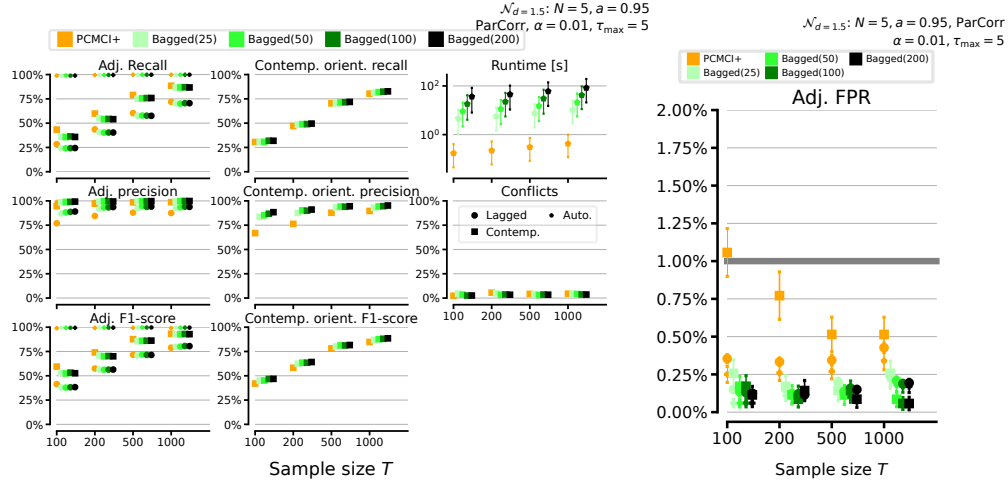


Figure 14: Numerical experiments with linear Gaussian setup for a varying time sample size.

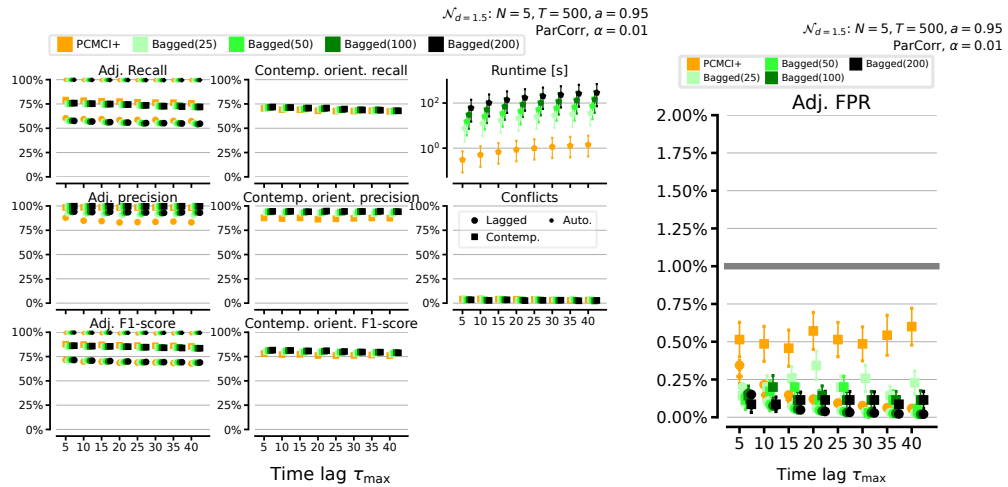


Figure 15: Numerical experiments with linear Gaussian setup for a varying maximum time lag.

Table 1: Mean absolute error (in %) between the bootstrapped confidence estimates and the estimated true link frequencies (extracted from Fig. 16).

|                         | $\alpha_{PC} = 10^{-2}$ | $\alpha_{PC} = 10^{-4}$ | $\alpha_{PC} = 10^{-5}$ |
|-------------------------|-------------------------|-------------------------|-------------------------|
| All absent links        | 2.7                     | 1.0                     | 1.3                     |
| All existing links      | 4.2                     | 3.2                     | 2.8                     |
| Contemp. absent links   | 4.7                     | 2.3                     | 2.5                     |
| Contemp. existing links | 7.8                     | 6.5                     | 5.1                     |
| Lagged absent links     | 2.2                     | 0.7                     | 0.9                     |
| Lagged existing links   | 1.8                     | 1.3                     | 1.5                     |

## S1.2 BAGGED-PCMCI+ CONFIDENCE MEASURE EVALUATION

Here we evaluate our proposed confidence measures for varying significance level  $\alpha_{PC}$  to study whether the bootstrapped confidence estimates approximate the estimated true link frequencies for  $\alpha_{PC} \rightarrow 0$  (Fig. 16). To reduce computational time, the setup here was slightly modified compared to the main text. While we used  $B = 1000$  and  $L = 3$  (number of cross-links) in the main body of the paper, here we set  $B = 250$  and  $L = 5$ . We vary  $\alpha_{PC}$  from 0.01 to  $10^{-5}$  to study the mean absolute error between the bootstrapped confidence estimates and the estimated true link frequencies.

We summarize the results regarding mean absolute error in Tab. 1. There does seem to be a decrease in error from  $\alpha_{PC} = 10^{-2}$  to  $\alpha_{PC} = 10^{-4}$  across all types of link frequencies, while there are mixed results for  $\alpha_{PC} = 10^{-5}$ . There is a visible recurrent positive bias for low values of the true frequencies (approximately 40-60%): The bootstrapped confidence measures tend to consistently overestimate the true link frequencies for this range. More research is needed to clarify whether the bootstrap confidence estimates do approximate the true link frequencies, or whether there are persistent biases. In this case a question would be, what this bias depends on (number of variables, graph structure, SCM properties, sample size, etc).

## 5.1 S1.3 EXPERIMENTS FOR BAGGED-PC

The previous numerical results have shown that the bagging approach leads to enhanced precision-recall when paired for PCMCI+. In order to demonstrate that this conclusion not only applies for PCMCI+ but also to other causal discovery methods, we carried out further experiments with the PC algorithm. That is, we combined our bagging approach with the PC algorithm (referred to as Bagged-PC) and compared its performance against the base PC algorithm. Both the base PC algorithm and Bagged-PC are adapted to time series as given in Runge [2020].

The results demonstrate that the gain using a bagging approach is similar here: Bagged-PC shows lower FPR and higher precision-recall compared to PC, especially for contemporaneous orientations (see Fig. 17 and Fig. 18). Hence, our results show that combining a causal discovery method with our bagging approach can considerably improve the performance compared to the base causal discovery method, albeit at the expense of increased computational runtime (if not parallelized).

## S2 DETAILS ON THE CONJECTURE OF ASYMPTOTIC CONSISTENCY

In section 3.3 of the main text, with **Conjecture 1** we conjecture that Bagged-PCMCI+ is asymptotically consistent under the assumptions formulated with **Assumptions 1**. Here, we give more details on this conjecture as well as on which step we are not yet able to prove.

To begin, note that **Assumptions 1** is almost equivalent to “Assumption 1” from Runge [2020]. The only difference is that **Assumption 1** from the main text requires the *Faithfulness Condition* Spirtes et al. [2000] whereas “Assumptions 1” from Runge [2020] requires the strictly weaker *Adjacency Faithfulness Condition* Ramsey et al. [2006]. In fact, we could modify **Assumption 1** to also require *Adjacency Faithfulness* instead of *Faithfulness*.

As proven in Runge [2020], the PCMCI+ algorithm is asymptotically consistent under “Assumptions 1” from Runge [2020]. Hence, PCMCI+ is also asymptotically consistent under **Assumption 1**.

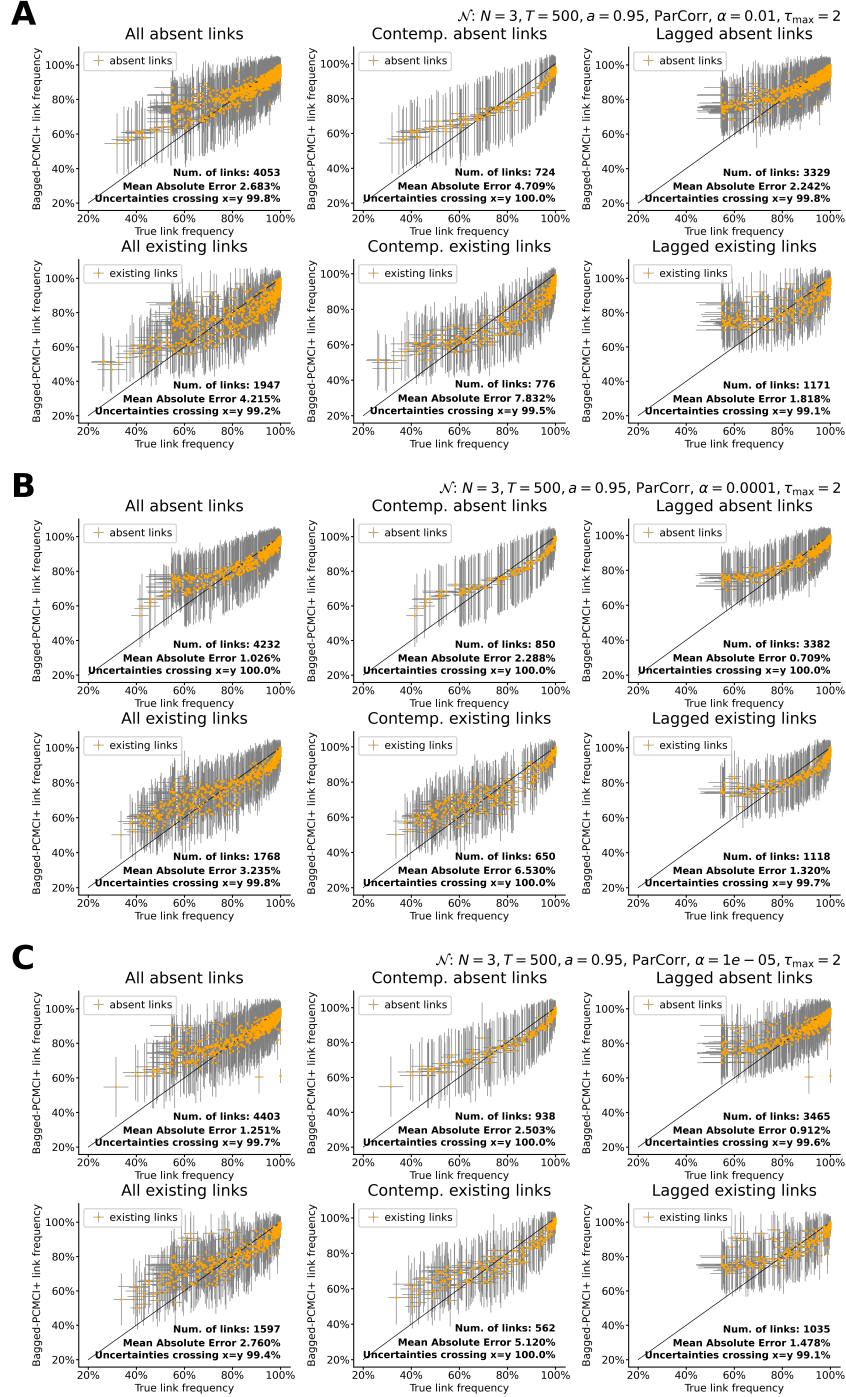


Figure 16: Estimated true link frequencies against mean Bagged-PCMC1+ link frequencies ( $B = 250$ ) for a linear Gaussian setup with parameters indicated at the top right. Grey bars indicate the one standard deviation error bars around the estimated value. The same model parameters are used in all three subfigures. Only the significance level  $\alpha_{PC}$  changes: (A)  $\alpha_{PC} = 0.01$ , (B)  $\alpha_{PC} = 10^{-4}$ , (C)  $\alpha_{PC} = 10^{-5}$ .

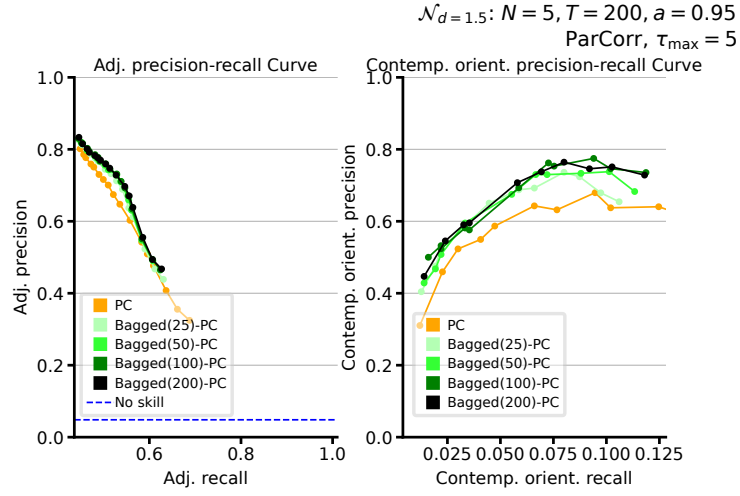


Figure 17: Precision-recall curves for adjacencies (left) and contemporaneous orientations (right) obtained by varying the significance level  $\alpha_{PC}$  in PC and Bagged-PC for the model setup as shown in the header. Results are shown for PC (orange line) and Bagged-PC with different numbers of bootstrap replicas  $B$  (lines with different shades of green). Here the PC algorithm is adapted for time series data.

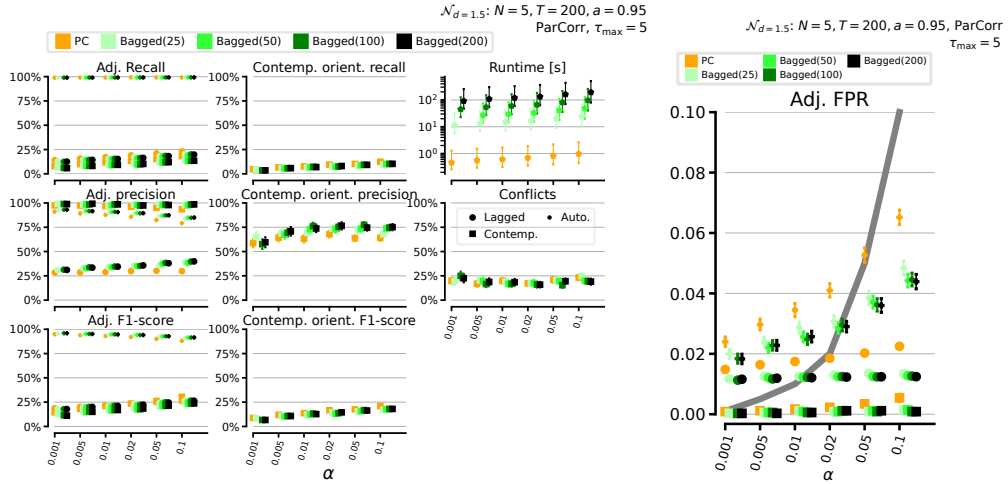


Figure 18: Numerical experiments with linear Gaussian setup for a varying  $\alpha_{PC}$  of PC. Here  $N = 5$ ,  $T = 200$ , and  $a = 0.95$ .

As explained in Section 3.2 of the main text, the output of Bagged-PCMCI+ is the graph obtained by a majority vote across all of the  $B$  bootstrap graphs that is cast individually for every pair of variables. Since every one of the  $B$  bootstrap graphs is the result of PCMCI+ on one of the bootstrap datasets and since PCMCI+ asymptotically returns the correct graph under **Assumption 1** (asymptotic consistency), it is tempting to conclude that all of the  $B$  bootstrap graphs asymptotically are the correct graph under **Assumption 1**. If this conclusion is true, then Bagged-PCMCI+ asymptotically returns the correct graph under **Assumption 1**, that is, then Bagged-PCMCI+ is asymptotically consistent under **Assumption 1**.

However, as thankfully pointed out to us by Tom Hochsprung, this line of reasoning might have a loophole: **Assumption 1** from the main text and “Assumptions 1” from Runge [2020] require *consistent conditional independence (CI) tests*. This assumption means that, asymptotically as the number of time steps and hence the number of samples used for CI testing goes to infinity, the CI tests make no errors. Making no errors means to always judge independence if, in fact, independence is true and to always judge dependence if, in fact, dependence is true. However, this assumption refers to the original dataset which is sampled from the true data-generating distribution. As opposed to that, the  $B$  bootstrap datasets are sampled from the empirical distribution defined by the original dataset. Consequently, the  $B$  bootstrap datasets are sampled from a different distribution than the original dataset. It is thus not immediately clear whether, when applied to a bootstrap dataset, the CI tests asymptotically always correctly detect (in-)dependence as defined by the true data-generating distribution. For example, even if in the true data-generating distribution independence holds, then for any finite number of time steps one almost surely has dependence in the empirical distribution defined by the original dataset. While the magnitude of this dependence in the empirical distribution converges to zero as the number of time steps goes to infinity, we have not yet proven that this fact implies that CI tests on the bootstrap datasets asymptotically correctly detect (in-)dependence as defined by the true data-generating distribution.

One way to tackle this could be to investigate the consistency for the limiting case that  $\alpha_{PC} \rightarrow 0$ . One hint that this could work is our finding in Tab. 1 that the mean absolute error between the bootstrapped confidence estimates and the estimated true link frequencies seems to partly converge.

Further, given the strong empirical performance of Bagged-PCMCI+ as seen in our numerical experiments, we conjecture that such an argument can finally be made and that, thus, Bagged-PCMCI+ is asymptotically consistent.

Moreover, we note that the above line of reasoning argues that asymptotically all of the  $B$  bootstrap graphs are the correct graph. While sufficient to get asymptotic consistency of Bagged-PCMCI+, this circumstance is stronger than needed: Even if not all of the  $B$  bootstrap graphs are asymptotically the correct graph, then Bagged-PCMCI+ might still recover the correct graphs by means of the majority vote. However, making an argument along these lines would require a significantly different proof.

Lastly, even if the conjecture of asymptotic consistency turns out to be false, then our extensive numerical experiments still demonstrate the usefulness of Bagged-PCMCI+ in the case of finite samples (that is, in the case of finitely many time steps).